THE JOURNAL OF COMPARATIVE NEUROLOGY 467:389–402 (2003)

Morphological Analysis of the Hyperpolarization-Activated Cyclic Nucleotide-Gated Cation Channel 1 (HCN1) Immunoreactive Bipolar Cells in the Rabbit Retina

IN-BEOM KIM, EUN-JIN LEE, TAE-HOON KANG, JIN-WOONG CHUNG, AND MYUNG-HOON CHUN*
Department of Anatomy, College of Medicine, The Catholic University of Korea, Seoul 137-701, Korea

ABSTRACT

Hyperpolarization-activated cation currents (I_h) have been identified in neurons in the central nervous system, including the retina. There is growing evidence that these currents, mediated by the hyperpolarization-activated cyclic nucleotide-gated cation channel (HCN), may play important roles in visual processing in the retina. This study was conducted to identify and characterize HCN1-immunoreactive (IR) bipolar cells by immunocytochemistry, quantitative analysis, and electron microscopy. The HCN1-IR bipolar cells were a subtype of OFF-type cone bipolar cells and comprised 10% of the total number of cone bipolar cells. The axons of the HCN1-IR cone bipolar cells ramified narrowly in the border of strata 1 and 2 of the inner plexiform layer (IPL). These cells formed a regular distribution, with a density of 1,825 cells/mm^2 at a position 1 mm ventral to the visual streak, falling to 650 cells/mm^2 in the ventral periphery. Double-labeling experiments demonstrated that their axons stratified narrowly within and slightly proximal to the OFF-starburst amacrine cell processes. In the IPL, they were presynaptic to amacrine cell processes. The most frequent postsynaptic dyads formed of HCN1-IR bipolar cell axon terminals are pairs composed of both amacrine cell processes. These results suggest that these HCN1-IR cone bipolar cells might be the same as the DAPI-Ba1 bipolar population, and might therefore be involved in a direction-selective mechanism, providing inputs to the OFF-starburst amacrine cells and/or the OFF-plexus of the ON–OFF ganglion cells. J. Comp. Neurol. 467:389–402, 2003.

Indexing terms: hyperpolarization-activated cyclic nucleotide-gated cation channel; cone bipolar cell; immunocytochemistry; electron microscopy; direction selectivity; rabbit retina

Bipolar cells convey signals from photoreceptors in the outer retina to amacrine and ganglion cells in the inner retina. In the mammalian retina, a single type of rod bipolar cell and multiple types of cone bipolar cells have been identified. Cone bipolar cells can be functionally divided into two types, ON and OFF, according to their response to light stimuli (Famiglietti and Kolb, 1976; Nelson and Kolb, 1983). ON and OFF cone bipolar cells are morphologically distinguished by the location of their terminal arbors in the inner plexiform layer (IPL): ON cone bipolar cells arborize in sublamina b (proximal half), whereas OFF cone bipolar cells arborize in sublamina a (distal half) of the IPL (Famiglietti and Kolb, 1976; Nelson et al., 1978; Euler and Wässle, 1995; Hartveit, 1997). Further, cone bipolar cells can be subdivided into several types according to their dendritic branching pattern, the

Grant sponsor: Ministry of Science and Technology in Korea; Grant number: Neurobiology Support M1-0108-00-0059.

*Correspondence to: Myung-Hoon Chun, Department of Anatomy, College of Medicine, The Catholic University of Korea, 505 Banpo-dong, Socho-gu, Seoul 137-701, Korea. E-mail: mhchun@catholic.ac.kr

Received 14 April 2003; Revised 14 July 2003; Accepted 29 July 2003
DOI 10.1002/cne.10957
Published online the week of October 27, 2003 in Wiley InterScience (www.interscience.wiley.com).

number of cones contacted, and the shape and stratification of their axon terminals in the IPL. Based on Golgi staining, nine types of cone bipolar cells have been described in the human retina (Kolb et al., 1992), nine in the monkey (Boycott and Wässle, 1991), 11 in the cat (Famiglietti, 1981; Kolb et al., 1981; Cohen and Sterling, 1990), and nine in the rabbit (Famiglietti, 1981). Recently, McGillem and Dacheux (2001) classified cone bipolar cells into 12 types using intracellular injection of fluorescent dye. However, Golgi staining and intracellular injection both have limitations: staining is random, capricious, and nonreproducible and does not allow the possibility of analyzing each type of cell throughout the whole retina.

Immunocytochemical approaches have been used to study various kinds of retinal neurons. Some antibodies label bipolar cell populations in the mammalian retina, in some cases together with other retinal neurons. An antibody raised against protein kinase C (PKC) labels rod bipolar cells in various mammalian species (Negishi et al., 1988; Greferath et al., 1990; Grünert and Martin, 1991; Young and Vaney, 1991; Chun et al., 1993). Antibodies against the calcium-binding protein recoverin label distinct populations of cone bipolar cells in different mammalian retinas (Milam et al., 1993; Chun et al., 1999) and reveal two types of cone bipolar cells in the rabbit (Massey and Mills, 1996) retina. Antisera raised against calbindin D-28K label bipolar cells along with other cell types in the monkey (Röhrenbeck et al., 1989; Grünert et al., 1994) and rabbit retina (Massey and Mills, 1996). Antibodies against CD15 label bipolar cells in some mammalian retinas (Andressen and Mai, 1997) and reveal a distinct type of cone bipolar cells in the rabbit retina (Brown and Masland, 1999). Most recently, antisera raised against the neurokinin 1 (NK1) receptor were shown to label another distinct type of cone bipolar cells in the rabbit retina (Casini et al., 2002). However, immunocytochemical markers for other populations of cone bipolar cells are still missing, although the antibodies described above are available as markers of bipolar cell populations in the rabbit retina. In addition, systematic investigations, using immunocytochemical markers, of the bipolar cell morphologies, spatial distributions, and synaptic circuitries in rabbit retina have remained elusive.

Hyperpolarization-activated cation currents (termed I_h, I_f, or I_q) have been identified in cardiac pacemaker cells (Brown et al., 1979; Yanagihara and Irisawa, 1980; DiFrancesco, 1981) and in neurons in the central and peripheral nervous systems (for review, see Pape, 1996), including the retina (Fain et al., 1978; Bader et al., 1979). Four members of a gene family encoding hyperpolarization-activated cyclic nucleotide-gated cation channels (HCN1–4) have recently been cloned (Gauss et al., 1998; Ludwig et al., 1998, 1999; Santoro et al., 1998; Seifert et al., 1999). Functional and morphological studies have demonstrated that I_h may play an important role in visual processing in the vertebrate retina. In retinal photoreceptors, I_h is activated during membrane hyperpolarization in response to bright light and moves the membrane potential closer to the depolarized "dark" level. Thus, the current provides an adaptive mechanism for the maintenance of synaptic transmission during strong light stimuli (Fain et al., 1978; Hestrin, 1987; Barnes and Hille, 1989). In addition, I_h plays a significant role in improving the temporal performance of visual signals in rods (Demontis et al., 1999) and bipolar cells (Gargini et al., 1999). Recently, morphological studies using in situ hybridization (Moosmang et al., 2001) and immunocytochemistry (Müller et al., 2001, 2003) showed that all four HCN channels are expressed in the rodent retina. Of those, HCN1 was highly expressed in the retina. In addition, Müller et al. (2001, 2003) have shown that a certain type of bipolar cell, as well as photoreceptors, some amacrine and ganglion cells, showed HCN1 immunoreactivity and, thus, an antibody against HCN1 could be used as a marker for identifying a certain type of bipolar cell in the retina.

Therefore, this study aimed to identify and characterize the bipolar cells showing HCN1 immunoreactivity in the rabbit retina. By using immunocytochemistry with a specific antibody against HCN1, we identified the HCN1-immunoreactive bipolar cells. They were further characterized using double-labeling, quantitative analysis, and electron microscopy.

MATERIALS AND METHODS

Tissue preparation

New Zealand rabbits weighing 2.0–2.5 kg were deeply anesthetized with ketamine (100 mg/kg) and xylazine (20 mg/kg). The eyes were enucleated and the animals were euthanized with an overdose of anesthetic. The animals were treated according to the regulations of the Catholic Ethics Committee of the Catholic University of Korea, Seoul, which conform to the National Institutes of Health (NIH) guidelines.

The anterior segments of the eyeballs were removed and the retinas were carefully dissected. The eyecups were fixed by immersion in fixative (4% paraformaldehyde + 0.2% picric acid or 4% paraformaldehyde + 0.05% glutaraldehyde in 0.1 M phosphate buffer (PB), pH 7.4), for 2–3 hours. Following fixation, the retinas were carefully dissected and transferred to 30% sucrose in PB for 24 hours at 4°C. They were then frozen in liquid nitrogen, thawed, and rinsed in 0.01 M PBS, pH 7.4.

Antibodies

A polyclonal antibody against a peptide (KPNSASNSRDDGNSVYPSK) that includes residues 6–24 in the N-terminus of rat HCN1 was purchased from Alomone Labs (Jerusalem, Israel, Cat. No. APC-056). This peptide sequence of the rat HCN1 channel shares high homology (84% identity) with that of the rabbit. The antibody is raised in rabbits and it was used at 1:500 dilution.

A polyclonal antiserum raised in rabbit (from Dr. K.-W. Koch, Institut für Informationsverarbeitung, Jülich, Germany) against recoverin (Lambrecht and Koch, 1992), which stains both OFF-type and ON-type cone bipolar cells in the rabbit retina (Massey and Mills, 1996), was used to compare them with a population of OFF-cone bipolar cells stained with HCN1 antiserum, used at 1:2,000 dilution.

Double-labeling immunofluorescence experiments were performed using the HCN1 antiserum in conjunction with the following two antibodies: a goat polyclonal antibody (Chemicon, Temecula, CA) against choline acetyltransferase (ChAT), which stains starburst cholinergic amacrine cells (Famiglietti, 1985a; Brandon, 1987; Famiglietti and Tumosa, 1987; Brown and Masland, 1999; Kim et al., 2000), used at 1:300 dilution, and a mouse monoclonal antibody (Sigma, St. Louis, MO) against protein kinase C

(PKC), which stains rod bipolar cells (Negishi et al., 1988; Greferath et al., 1990; Young and Vaney, 1991; Chun et al., 1993; Strettoi and Masland, 1995), used at 1:1,000.

Immunocytochemistry

Retinal whole-mount preparations, and 40-μm-thick vertical and horizontal vibratome sections were used. The retinas were incubated in 10% normal goat serum (NGS) and 1% Triton X-100 in PBS for 1 hour at room temperature to block nonspecific binding sites. They were then incubated with the rabbit polyclonal antibodies directed against HCN1 or recoverin in PBS containing 0.5% Triton X-100 for 13 days at 4°C. Retinas were washed in PBS for 45 minutes (3 × 15 minutes), incubated for 2–12 hours in peroxidase-conjugated goat antirabbit IgG (Jackson ImmunoResearch, West Grove, PA; dilution 1:100) or in Cy3-conjugated goat antirabbit IgG (Jackson ImmunoResearch; dilution 1:500) with 0.5% Triton X-100 at 4°C, and rinsed in PBS. The tissues were further washed in 0.1 M Tris buffer (pH 7.6) for 45 minutes (3 × 15 minutes), preincubated in 0.05% 3,3′-diaminobenzidine tetrahydrochloride (DAB) in 0.1 M Tris buffer for 10 minutes, and incubated in the same solution containing 0.05% hydrogen peroxide (H_2O_2) for an additional 10 minutes. Subsequently, the retinas were washed in PB, mounted on gelatin-coated slides with the ganglion cell layer (GCL) facing upwards, and coverslips were applied with Vectashield (Vector Laboratories, Burlingame, CA). Specificity of immunostaining was evaluated by omitting the incubation step with the primary antiserum.

For double-labeling, whole mounts and sections were incubated for 1–3 days in a mixture of HCN1 antibody and one of the other antibodies diluted in PBS containing 0.5% Triton X-100 in PB at 4°C. The retinas were rinsed for 30 minutes with PBS and incubated in the presence of appropriate secondary antibodies conjugated with Alexa Fluor 488 (Molecular Probes, Eugene, OR) or with Cy3 (Jackson ImmunoResearch) at a dilution of 1:200 in PBS containing 0.5% Triton X-100 in PB at 4°C for 2–4 hours at room temperature. They were then washed for 30 minutes with PB and coverslipped. To ensure that the secondary antibody had not crossreacted with the inappropriate primary antibody, some control sections were incubated in rabbit polyclonal primary antibody followed by antimouse secondary antibody, and other sections were incubated in mouse primary antibody followed by antirabbit secondary antibody. These sections did not show any immunostaining.

Confocal microscopy

All fluorescent specimens were analyzed using a Bio-Rad Radiance Plus (Bio-Rad, Hemel Hempstead, UK) confocal scanning microscope, installed on a Nikon Eclipse E600 fluorescence microscope (Nikon, Tokyo, Japan). Alexa Fluor 488 and Cy3 signals were always detected separately. The Alexa Fluor 488 labeling was excited using the 488-nm line of an argon ion laser and detected after passing a HQ513/30 emission filter (Bio-Rad). For detection of the Cy3 signal, the 543-nm wavelength of a green helium–neon laser was used in combination with a 605/32 emission filter (Bio-Rad). Images were imported into Adobe PhotoShop v. 5.5 (Adobe Systems, Mountain View, CA) and photographed onto slide film (Kodak Ektachrome 100; Eastman Kodak, Rochester, NY). For presentation, all manipulations (brightness and contrast only) were carried out equally.

Quantitative analysis

Quantitative evaluation of the HCN1-immunoreactive (IR) bipolar cells was performed on horizontal sections and retinal whole mounts. Cell density was expressed as the number of HCN1-IR bipolar cells per square millimeter of retinal surface. Nearest-neighbor analysis (Wässle and Riemann, 1978) was performed for each retina on the same fields used for calculating HCN1-IR bipolar cell densities. The distribution of nearest-neighbor distances was compared with the normal Gaussian distribution expected for the same values of the mean and standard deviation of the nearest-neighbor distances. The results were not corrected for shrinkage of the tissue during the mounting process, because this was negligible.

Electron microscopy

Rabbits were anesthetized and euthanized as described above. The eyecups were fixed in a mixture of 4% paraformaldehyde + 0.05–0.1% glutaraldehyde in PB for 30 minutes at room temperature. The retinas were then carefully dissected; small pieces were taken from the central region and fixed for an additional 2 hours at 4°C. After being washed in PB, the retinal pieces were transferred to 30% sucrose in PB for 6 hours at 4°C, rapidly frozen in liquid nitrogen, thawed, and embedded in 4% agar in distilled water. The retinal pieces were cut at 40 μm using a vibratome and sections were placed in PBS. They were incubated in 10% NGS in PBS for 1 hour at room temperature to block nonspecific binding and were then incubated in HCN1 antibody for 12 hours at 4°C.

The following immunocytochemical procedures were carried out at room temperature. The sections were washed in PBS for 45 minutes (3 × 15 minutes), incubated in biotin-labeled goat antirabbit IgG (Jackson ImmunoResearch; dilution 1:100) for 2 hours, and then washed three times in PBS for 45 minutes (3 × 15 minutes). The sections were then incubated in avidin-biotin-peroxidase complex (ABC) solution (Vector Laboratories) for 1 hour, washed in TB, and then incubated in 0.05% DAB solution containing 0.01% H_2O_2. The reaction was monitored using a low-power microscope and was stopped by replacing the DAB and H_2O_2 solution with TB.

The stained sections were postfixed in 1% glutaraldehyde in PB for 1 hour and, after washing in PB containing 4.5% sucrose for 15 minutes (3 × 5 minutes), they were postfixed in 1% OsO_4 in PB for 1 hour. Afterwards they were rewashed in PB containing 4.5% sucrose and dehydrated in a graded series of alcohol. During the dehydration procedure, they were stained en bloc with 1% uranyl acetate in 70% alcohol for 1 hour, then transferred to propylene oxide and flat-embedded in Epon 812. After curing at 60°C for 3 days, well-stained areas were cut out and attached to an Epon support for further ultrathin sectioning (Reichert-Jung, Nuβloch, Germany). Ultrathin sections (70–90 nm thick) were collected on one-hole grids

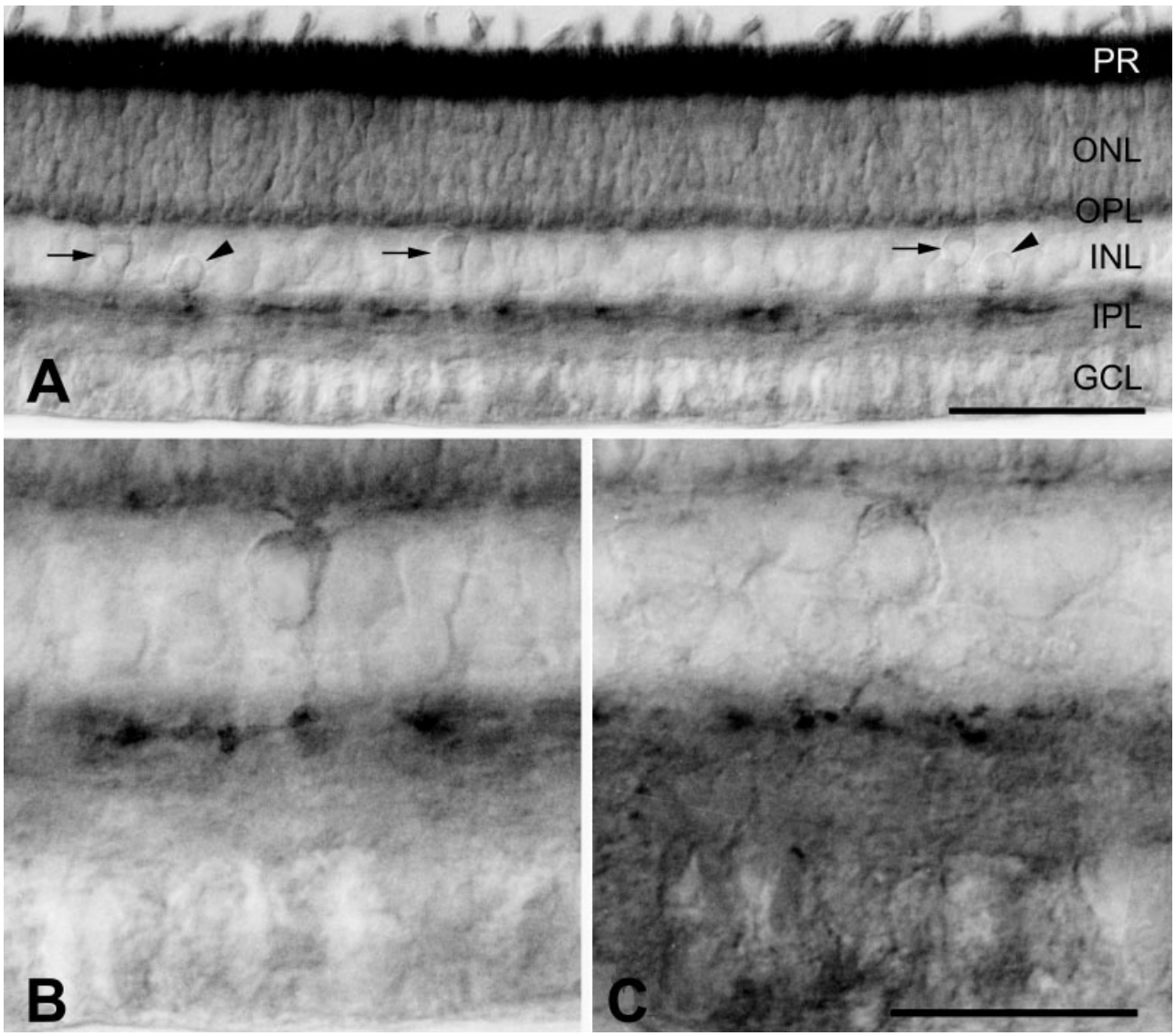

Fig. 1. Light photographs taken from 40-μm-thick vertical vibratome sections of the rabbit retina processed for HCN1 immunoreactivity. **A:** Immunoreactivity is seen in three bipolar cell somata (arrows) and two somata of amacrine cells (arrowheads) located in the inner nuclear layer (INL). One prominent band of labeled processes is visible in the border of strata 1 and 2 of the inner plexiform layer (IPL). The outer and inner segments of the photoreceptors (PR) show strong immunoreactivity. The outer nuclear layer (ONL) and the outer plexiform layer (OPL) also show weak immunoreactivity. **B,C:** Two examples of HCN1-IR bipolar cells are clearly seen. B: The soma of an HCN1-IR bipolar cell is located in the distal half of the INL. Three dendrites originated from the soma run horizontally within the OPL, and its axon descends toward GCL and ramifies flat in the border of strata 1 and 2 of the IPL. Lobular terminals of the axon are clearly seen. C: The soma of an HCN1-IR bipolar cell is located in the level similar to that shown in B. Two dendrites originating from the soma are clearly seen. An axon descends through INL, branches into two secondary axons near IPL, and ramifies flat at the same level as does the axon of a HCN1-IR bipolar cell shown in A. GCL, ganglion cell layer. Scale bars = 50 μm in A; 25 μm in C.

coated with Formvar and examined using an electron microscope (Jeol 1200EX, Tokyo, Japan).

RESULTS

HCN1 immunostaining patterns

Immunoreactivity was found in the outer and inner segments, in somata of the outer nuclear layer (ONL), the inner nuclear layer (INL) and the ganglion cell layer (GCL), and in processes in the outer plexiform layer (OPL) and the inner plexiform layer (IPL) (Fig. 1). In the INL, one type of HCN1-immunoreactive (IR) soma was located in the distal INL near OPL, and the other was in the proximal INL adjacent to the IPL (Fig. 1). In the IPL, strong IR processes were observed mainly in the border of strata 1 and 2 of the IPL, and weak immunoreactive processes were found occasionally through strata 3–5. Each labeled bipolar cell soma in the distal INL gave rise to fine processes that ascended to the OPL and to a single smooth process that descended toward the GCL, branched

and ramified in the border of strata 1 and 2 of the IPL as lobular terminals (Fig. 1). Each amacrine cell soma in the proximal INL appeared to have a primary dendrite, branching into secondary dendrites that distributed in the border of strata 1 and 2 of the IPL (Fig. 1), although it was difficult to trace its processes because of its weak immunoreactivity. These observations indicate that HCN1-IR bipolar and amacrine cell populations are present in the rabbit retina. Labeled somata were also observed in the GCL, but rarely (Fig. 2D).

Morphology of HCN1-IR bipolar cells

HCN1-IR bipolar cells were observed in all retinal regions. Their dendritic arborizations in the OPL were characterized by intensely immunoreactive puncta and their axonal processes, emerging from large somata, passed through the INL and generally branched and ramified narrowly in the border of strata 1 and 2 of the IPL (Fig. 1B,C). Prominent lobular terminals along the axonal processes were clearly visible. To investigate dendritic and axonal arborization and distribution of the soma of HCN1-IR bipolar cells horizontally, attempts were first made to immunostain whole retinas. However, satisfactory immunostaining could not be achieved, presumably because of lack of penetration of the HCN1 antibody. Thus, immunostaining was performed on the horizontal sections through the retina. In horizontal sections, arborizations of the HCN1-IR bipolar cells could be observed in detail both in the OPL and in the IPL (Fig. 2A–C). In the OPL, the dendritic processes were thin, extended radially, and joined with dendrites from neighbors, but they appeared not to overlap each other significantly (Fig. 2A). These dendrites emerged from HCN1-IR bipolar somata, which appeared to form a regular mosaic (Fig. 2B). In the IPL, it was not possible to define axonal arbors of individual HCN1-IR bipolar cells because the immunoreactive processes with lobular terminals joined together and formed a continuous beaded meshwork (Fig. 2C).

Characterization of HCN1-IR bipolar cells

The HCN1-IR bipolar cells arborize in the sublamina a of the IPL, and thus belong to OFF-type cone bipolar cells. To determine whether these cells constitute a unique OFF-type cone bipolar cell population, HCN1-IR bipolar cells were compared with recoverin-IR OFF cone bipolar cells (Massey and Mills, 1996), which are only one of the OFF-type cone bipolar cells that can be identified immunocytochemically in the rabbit retina. Unfortunately, double-labeling experiments could not be performed because antibodies against HCN1 and recoverin were developed from the same kind of host. Thus, different vertical sections were processed for HCN1 and recoverin immunoreactivities (Fig. 2D,E).

Recoverin immunoreactivity was found in photoreceptors and in two types of bipolar cells with two broad bands of terminals in the IPL: one in sublamina a, and the other in sublamina b (Fig. 2E), in accordance with a previous report (Massey and Mills, 1996). The former originated from OFF-type cone bipolar cells. The somata of recoverin-IR OFF cone bipolar cells were located in a more proximal portion of the distal half of the INL (Fig. 2E) than the HCN1-IR bipolar cell somata (Fig. 2D). The dendrites of recoverin-IR OFF cone bipolar cells could not be observed because of the intense staining of the OPL; their axonal processes passed through the INL and branched and ramified broadly through strata 1 and 2 of the IPL (Fig. 2E), while the axon of the HCN1-IR bipolar cell descended and terminated, forming a very narrow band with lobular terminals in the border of strata 1 and 2 of the IPL (Fig. 2D). Although a comparison could not be achieved directly in the same section, the difference of axonal morphologies between recoverin-IR OFF cone bipolar cell and HCN1-IR bipolar cell suggests that HCN1-IR bipolar cells are a type of OFF cone bipolar cells distinct from the recoverin-IR OFF cone bipolar cells.

In this study, HCN1-IR bipolar cell axons ramifying in the border of strata 1 and 2 of the IPL were observed. This stratification level corresponds to that of processes of the OFF-starburst amacrine cells (Famiglietti, 1983; Famiglietti and Tumosa, 1987; Vaney, 1990), OFF-processes of the ON–OFF ganglion cells (Amthor et al., 1984, 1989; Yang and Masland, 1994), and distal processes of the DAPI-3 amacrine cells (Vaney, 1990; Wright et al., 1997). We therefore performed double-labeling experiments with an antibody against HCN1 and an antibody against ChAT, which labels cholinergic starburst amacrine cells. The vertical section shown in Figure 3A was processed for HCN1 immunoreactivity and the section in Figure 3B was processed for ChAT. As seen in a merged confocal image of a vertical section in Figure 3C, the processes of the HCN1-IR bipolar cells were found to stratify narrowly within and slightly proximal to the OFF-starburst amacrine cell processes. In a merged confocal image of a horizontal section in Figure 3F, the processes of the HCN1-IR bipolar cells follow OFF-starburst amacrine cell processes, suggesting that both processes are costratified and cofasciculated. In particular, all lobular terminals (small arrows in Fig. 3C,F) of the HCN1-IR bipolar cells were within the band of OFF-starburst amacrine cell processes. These results suggest that HCN1-IR bipolar cells make contacts with OFF-starburst amacrine cells.

Quantitative analysis of HCN1-IR bipolar cell population

For quantitative analysis, the areas along the dorsal to ventral strips, including or just near the optic disc through the ventral retina were sampled in 3-mm steps from three retinas. Incomplete staining of the whole mounts did not allow imaging of the whole mosaic including the dendrites, somata, and axons.

To compare the density of HCN1-IR bipolar cells with that of rod bipolar cells, several retinal samples double-labeled with antibodies against HCN1 and PKC were prepared. Colocalization was not observed, and the HCN1-IR bipolar cells and rod bipolar cells thus comprise separate populations (Fig. 3G–I). In these samples, both the HCN1-IR bipolar cells and the rod bipolar cells were counted. The density of the rod bipolar cells was close to those of previous reports (Young and Vaney, 1991; Strettoi and Masland, 1995) and decreased with increasing eccentricity, as would be expected. The ratio of HCN1-IR bipolar cells to rod bipolar cells was constant across eccentricities (Fig. 4A). Combined with data by Strettoi and Masland (1995) showing that in representative regions of the retina all the bipolar cells as well as the fraction accounted for by rod bipolar cells were counted, these results suggest that HCN1-IR bipolar cells comprise 10% of the total cone bipolar cells of the ventral rabbit retina.

The density of HCN1-IR bipolar cells was 1,825 cells/mm^2 at a position 1 mm ventral to the visual streak,

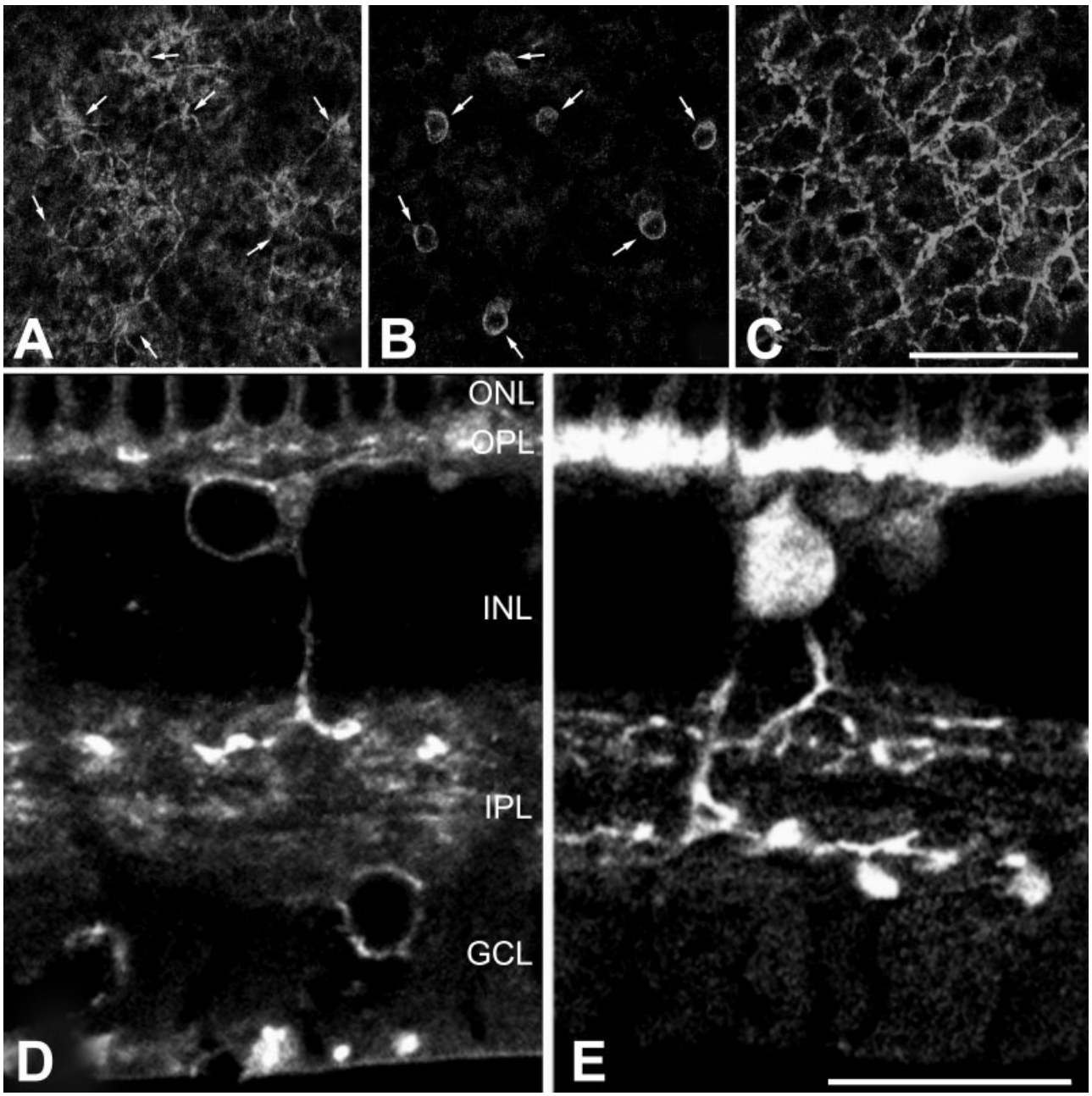

Fig. 2. Confocal micrographs taken at different focal planes in the same (A,B) and similar (C) fields of horizontal sections processed for HCN1 immunoreactivity and taken from vertical vibratome sections processed for HCN1 (D) and recoverin (E) immunoreactivities. The field is taken from the mid-ventral retina. **A:** The focus is on the OPL, and dendrites originating from the soma shown in B are visible. Small arrows indicate the location of the soma shown in B. The staining of this mosaic of brightly labeled dendrites is incomplete, but they appear not to overlap each other significantly. **B:** The focus is on the distal INL. Seven HCN1-IR bipolar somata (small arrows) showing strong immunoreactivity form a regular mosaic. **C:** The focus is on sublamina a of the IPL. A dense plexus of labeled processes with lobular terminals can be seen. It has a continuous beaded-meshwork appearance. **D:** A soma of an HCN1-IR bipolar cell is located in the distal half of the INL and its dendrites obliquely ascend toward the OPL. The axon of the HCN1-IR bipolar cell descends and terminates, forming a very narrow band with lobular terminals in the border of strata 1 and 2 of the IPL. E: An OFF-type recoverin-IR bipolar cell soma is located in a more proximal region of the INL than is the HCN1-IR bipolar cell shown in D. Its dendrites are not visible because of very intense staining of the OPL. The axon of the OFF-type recoverin-IR bipolar cell descends toward the GCL and branches into secondary axons near the border of the INL and IPL. Secondary axons branch into tertiary or more forms and finally form a broad band through strata 1 and 2 of the IPL. Scale bars = 50 μm in C; 20 μm in E.

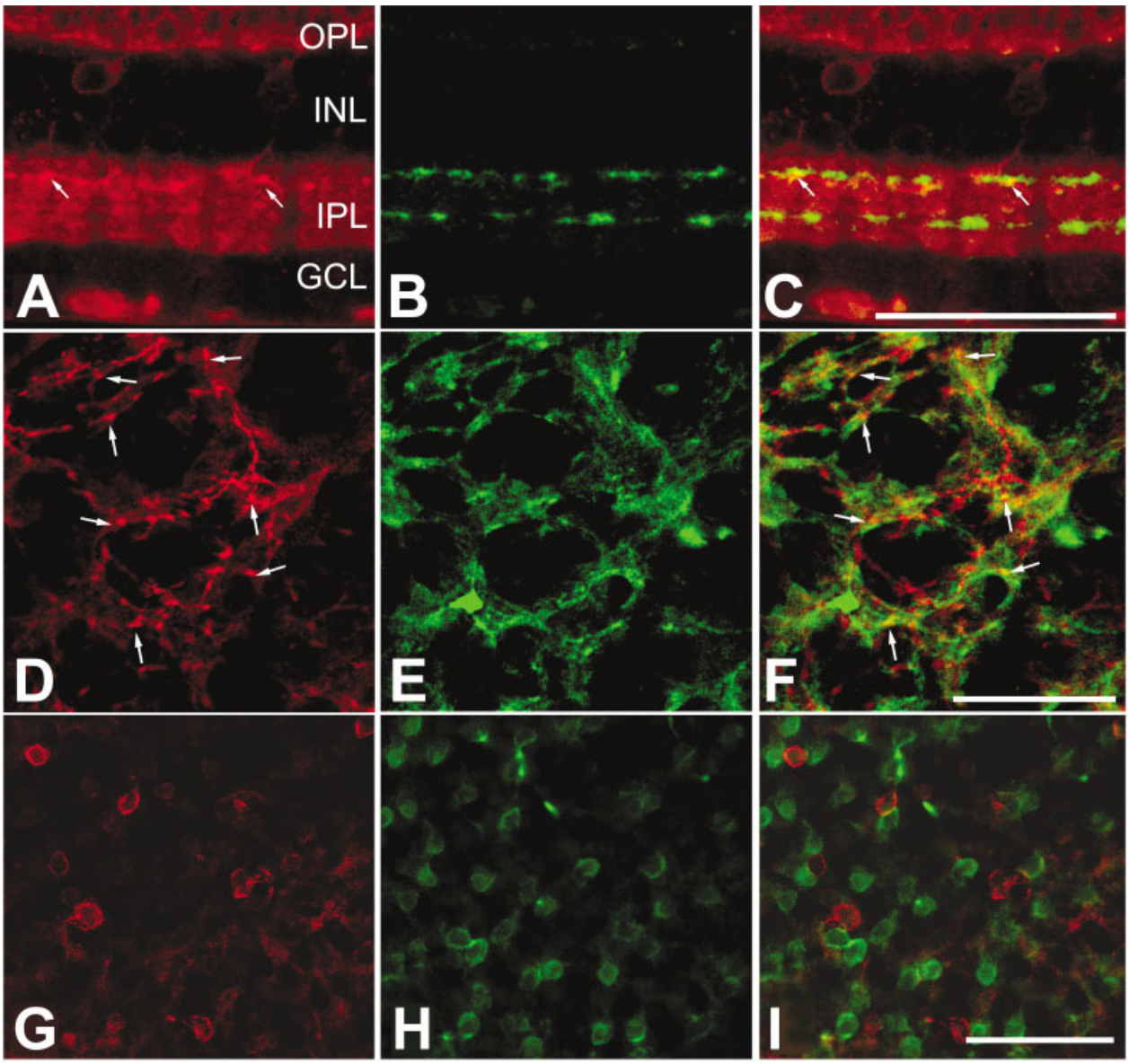

Fig. 3. Confocal micrographs taken from vertical vibratome sections (A–C) and a retinal whole mount (D–F) processed for HCN1 (A,D) and ChAT (B,E) immunoreactivities and taken from a horizontal vibratome section (G–I) processed for HCN1 (G) and PKC (H) immunoreactivities. HCN1 immunoreactivity was visualized using a Cy3-conjugated secondary antibody (red); ChAT or PKC immunoreactivity was visualized using an Alexa 488 Fluor-conjugated secondary antibody (green). **A,B:** In A, two HCN1-IR bipolar cell somata are visible in the INL and their processes are stratified in sublamina a of the IPL. Small arrows indicate lobular terminals of the HCN1-IR bipolar cell axons. In B, starburst cholinergic amacrine processes stratify in sublaminae a and b of the IPL, forming two prominent bands. **C:** In this merged image of A and B, the HCN1-IR bipolar cell axons are observed to stratify narrowly within and slightly proximal to the OFF-band of starburst amacrine cell processes. Note that lobular terminals (small arrows) of the HCN1-IR bipolar cell axons are situated within the band of OFF-plexus of the starburst amacrine cells. **D,E:** The focus is on sublamina a of the IPL. In these confocal images of a retinal whole mount, the pattern of the plexus formed by HCN1-labeled processes (D) and that of the OFF-plexus of the starburst amacrine cells (E) are seen. **F:** In this merged image the HCN1-IR processes follow the OFF-plexus of the starburst amacrine cells. All lobular terminals (small arrows) of the HCN1-IR bipolar cells shown in D lie on the OFF-plexus of the starburst amacrine cells, whereas processes of the OFF-type starburst amacrine cells, not superimposed with HCN1-labeled processes, can be seen. **G,H:** In G, several HCN1-IR bipolar cell somata are visible and numerous PKC-labeled rod bipolar cell somata are clearly seen in H. **I:** In this merged image of G and H, HCN1-IR bipolar cell somata never demonstrate PKC immunoreactivity. Scale bars = 50 μm in C,I; 20 μm in F.

decreased with increasing eccentricity, and reached 650 cells/mm^2 at a position 13 mm ventral periphery in this study (Fig. 4B). In Figure 4B, the peak density was estimated at about 2,200 cells/mm^2 at the visual streak. Nearest-neighbor analysis (Wässle and Riemann, 1987) was performed at a position 6 mm ventral to the optic disc to assess the distribution pattern of the somata of HCN1-IR bipolar cells (Fig. 4C). The resulting histogram (Fig. 4C) shows that HCN1-IR bipolar cells were nonrandomly distributed across the retina. The ratio between the

mean and the standard deviation of the nearest-neighbor distance is an index of mosaic regularity (Wässle and Riemann, 1987): the higher this ratio, the greater the regularity. For the HCN1-IR bipolar cell population in this region, the ratio was 3.6.

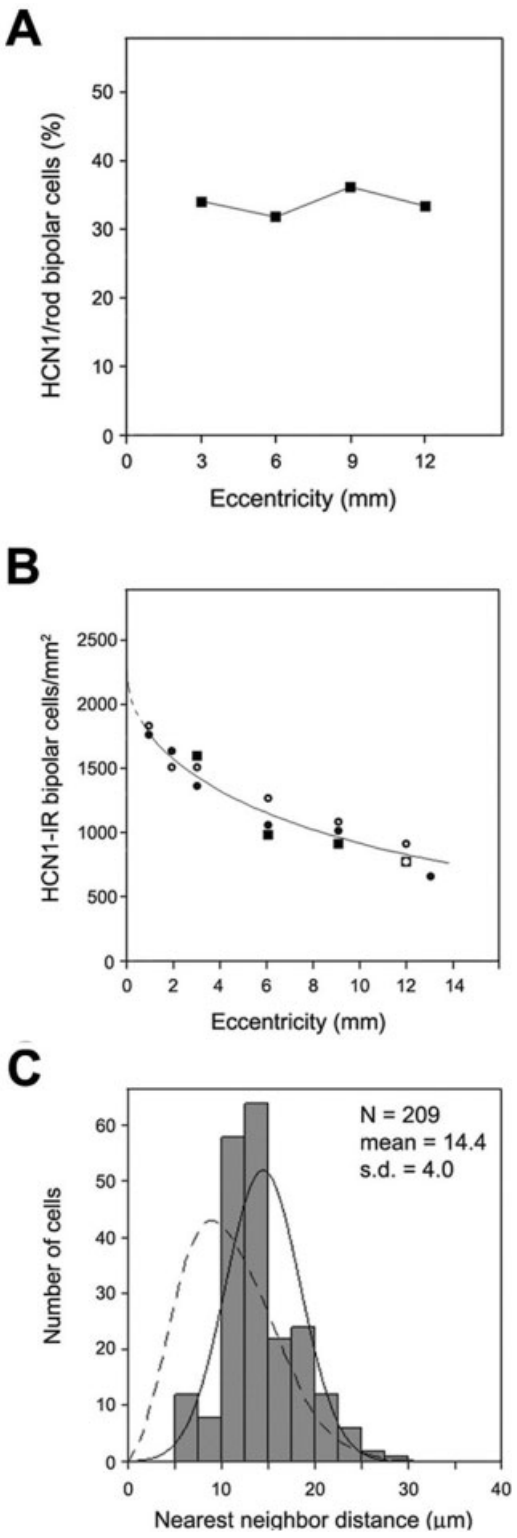

In horizontal sections of the retina, the dendrites and axons of the HCN1-IR bipolar cells appeared to tile the retina, probably with overlap (Fig. 2A–C). It was impossible to judge the degree of overlap and to accurately define dendritic and axonal arbors of individual HCN1-IR bipolar cells. In the rabbit retina, the dendrites and axon terminals of other bipolar cells show territorial behavior and therefore their dendritic and axonal field coverage approaches unity (Young and Vaney, 1991; Mills and Massey, 1992; Brown and Masland, 1999). Thus, on the assumption that the HCN1-IR bipolar cells follow this rule, the dendrite and axon diameter can roughly be estimated from the density of their somata. For HCN1-IR bipolar cells, their dendritic and axonal fields are 25 μm in diameter near the visual streak and 40 μm at the ventral periphery.

Synaptic connectivity of the HCN1-IR bipolar cells

Because HCN1 is an integral membrane protein, one would expect HCN1 immunoreactivity localized to cell membranes. However, it was identified as an electron-dense reaction product closely associated with the cytoplasmic matrices and synaptic vesicles as well as cell membranes. We have previously explained this discrepancy (Kim et al., 2002) as an artifact that frequently occurs in ultrastructurally localizing integral membrane proteins such as GABA transporters and glutamate receptors (Ribak et al., 1996; Brandstätter and Hack, 2001), and that might be attributed to preembedding techniques in immunocytochemistry.

Figure 5A shows an ultrathin section through the OPL taken from the rabbit retina processed for HCN1 immunoreactivity. Labeled bipolar cell dendrites running across the region occupied by the large processes of horizontal cells were observed displaying relatively strong immunoreactivity. They terminate in close association with the vitreal surface of the cone pedicle (CP) and make basal contacts (arrows). Thus, HCN1-IR bipolar cells belong to OFF-type cone bipolar cells.

In the IPL, HCN1-IR bipolar cell axons can be easily identified by their dense peroxidase reaction products, synaptic ribbons, and postsynaptic densities. Amacrine and ganglion cell processes were identified according to ultrastructural criteria (Dubin, 1970; Kolb, 1979; McGuire et al., 1984, 1986). Thus, processes that contained synaptic vesicles and made conventional chemical output synapses were considered amacrine cell processes, and pro-

Fig. 4. **A:** The ratio of HCN1-IR bipolar cells to rod bipolar cells across eccentricities. The graph shows that the ratio of HCN1-IR bipolar cells to PKC-IR rod bipolar cells remains constant across eccentricities. **B:** Distribution of HCN1-IR bipolar cells across eccentricities. The graph shows the variation in HCN1-IR bipolar cell density as a function of vertical strips through the ventral retina. Seventeen regions from two retinas were sampled. **C:** Nearest-neighbor analysis of the HCN1-IR bipolar cell population in the INL. The histogram for the HCN1-IR bipolar cell population (bars) is relatively well matched by a Gaussian curve (solid line), which represents a regular cell distribution, but is not well matched by a Poisson curve (dotted line), which represents a random cell distribution. The histogram shows the number of cells in the sample (N), the mean distance between cells (mean), and the standard deviation (s.d.). The field used for the analysis was located 6 mm ventral to the optic nerve head.

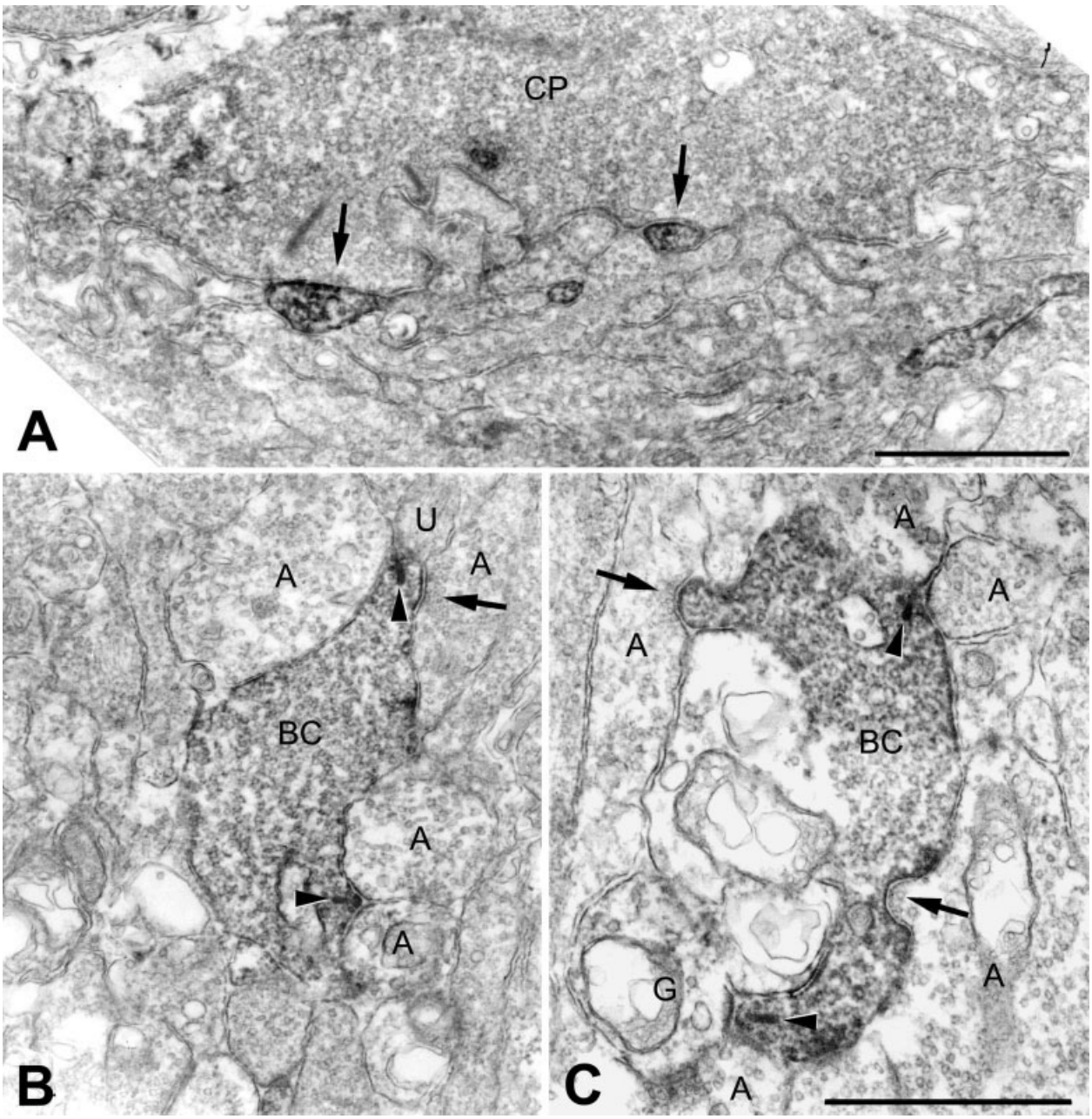

Fig. 5. **A:** Electron micrograph showing the connections of the HCN1-IR bipolar cells in the OPL. In the OPL, dendrites of HCN1-IR bipolar cells establish basal contacts (arrows) with the cone pedicle (CP). On the right, a labeled dendrite receiving synaptic input from a putative inter-plexiform cell process is seen. **B,C:** Electron micrographs showing output synapses of HCN1-IR bipolar cells onto dyads including amacrine cell component in sublamina a of the IPL. B: An axon terminal of a HCN1-labeled cone bipolar cell process (BC) makes two ribbon synapses (arrowheads) onto two postsynaptic dyads: one consists of both amacrine cell processes (A), and the other consists of an amacrine (A) and an unidentified (U) processes. In the upper part, the axon terminal receives a synaptic input (arrow) from another amacrine cell process (A). C: Two postsynaptic dyads at the ribbon synapses (arrowheads) are seen; one is comprised of two amacrine processes (A), and the other one of an amacrine cell process and a ganglion cell dendrite (G). The labeled bipolar axon terminal (BC) receives synaptic inputs (arrows) from two different amacrine cell processes (A). Scale bars = 0.5 μm.

cesses that contained microtubules instead of synaptic vesicles were classified as ganglion cell dendrites. The labeled axons were found in or near the interface of strata 1 and 2 of the IPL (15–28% of the distance from the INL to the GCL). As expected from light microscopy, other HCN1-IR amacrine cell processes were also seen at this depth in the IPL, but they are not described further here.

Figure 5B,C was taken from the border of strata 1 and 2 of the IPL. Figure 5B shows an HCN1-IR cone bipolar cell axon terminal (BC) densely filled with synaptic vesi-

cles and displaying homogeneous labeling. The labeled bipolar axon terminal makes two ribbon synapses (arrowheads); one dyad consists of two unlabeled amacrine cell processes (A), and the other consists of an unlabeled amacrine cell process (A) and an unlabeled unidentified cell process (U). This labeled bipolar axon terminal receives a synaptic input (arrow) from an unlabeled amacrine cell process (A). In Figure 5C, two postsynaptic dyads opposed to the HCN1-IR bipolar axon terminal (BC) are observed at ribbon synapses (arrowheads). One dyad is a pair of unlabeled amacrine cells (A) and the other comprises an unlabeled amacrine cell (A) and an unlabeled ganglion cell (G). This labeled bipolar axon terminal receives synaptic inputs (arrows) from two different unlabeled amacrine cell processes (A), similar to that in Figure 5B.

Figure 6A shows another example of a ribbon synapse (arrowhead), where an unlabeled amacrine (A) and an unlabeled ganglion cell process (G) comprise a postsynaptic dyad. Figure 6B shows an example of a ribbon synapse (arrowhead), where a labeled amacrine (A+) and an unlabeled ganglion cell process (G) comprise a postsynaptic dyad. Figure 6C shows an axon terminal of the HCN1-IR cone bipolar cell (BC) making a ribbon synapse (arrowhead) onto two unlabeled ganglion cell processes (G). Figure 6D shows an example of a rarely observed ribbon synapse (arrowhead), where the unlabeled amacrine cell process (A) comprises a monad. However, it cannot be excluded that this monad resulted from the plane of section.

Quantitative analysis of the synaptic circuitry of the HCN1-IR bipolar cells

A total of 237 synapses were identified in the IPL; 60 were inputs from amacrine cell processes and 177 were output synapses onto amacrine, ganglion, and unidentified cell processes. At the light microscopic level, HCN1-IR amacrine cell processes appeared to ramify at the same level of the IPL as HCN1-IR bipolar cell axons, and at the electron microscopic level labeled processes that appeared to belong to amacrine cells were observed. Thus, synapses between labeled bipolar cell processes and labeled amacrine cell processes were expected. However, these were rare: only one was observed out of 60 input synapses and only two out of 177 output synapses. These synapses made by HCN1-IR bipolar cells in the IPL are summarized in Table 1.

A total of 60 amacrine cell processes, which are presynaptic to HCN1-IR cone bipolar cells, were observed. All but one of these (98.3%) were unlabeled amacrine cells, and among these, eight amacrine processes (13.6%) gave synaptic input onto HCN1-IR cone bipolar cells in a reciprocal manner. Only one instance (1.7%) was observed of a labeled bipolar cell process receiving a synaptic input from an HCN1-labeled amacrine cell process. Among the presynaptic amacrine cell processes, some processes probably belonged to AII amacrine cells, as judged by their cytological characteristics (Strettoi et al., 1992; Chun et al., 1993). However, putative AII processes were fewer than expected, and the exact number of AII amacrine cell processes could not be determined in this study.

Of the postsynaptic elements at the ribbon synapses of the HCN1-IR cone bipolar cells, the most frequent postsynaptic dyads (87/169, 51.4%) consisted of two unlabeled amacrine cell processes (A–/A–). Dyads (38/169, 22.5%) consisting of an unlabeled amacrine process and a ganglion cell dendrite (A–/G), and dyads (25/169, 14.8%) comprising an unlabeled amacrine process and an unidentified process (A–/U) followed. In these HCN1-IR bipolar cells, dyads containing a ganglion cell dendrite were fewer than those containing an amacrine cell process, and thus dyads comprising G/G (4 cases, 2.4%) and G/U (10 cases, 5.9%) were rare. As described above, postsynaptic dyads containing HCN1-labeled amacrine process were observed in only two cases (1.2%).

DISCUSSION

In this study, we identified and characterized HCN1-IR bipolar cells in the rabbit retina using immunocytochemistry, quantitative analysis, and electron microscopy. The HCN1-IR bipolar cells are a subtype of OFF-type cone bipolar cells and make up 10% of the cone bipolar cells in the rabbit retina. Their axons stratify flat in the border of strata 1 and 2 of the IPL, and within and slightly proximal to the OFF-starburst amacrine cell processes. The HCN1-IR bipolar cells form a regular distribution, with a peak density of 1,825 cells/mm^2 near visual streak falling to 650 cells/mm^2 in the ventral periphery. Their axon terminals receive synaptic input from unlabeled amacrine processes and their major output targets are dyads composed of both amacrine cell processes.

Characterization of HCN1-IR cone bipolar cells

Cone bipolar cells can be functionally divided into ON- and OFF-types, according to their response to light stimuli (Famiglietti and Kolb, 1976; Nelson and Kolb, 1983). They are morphologically distinguished by the location of their terminal arbors in the IPL: ON-types arborize in sublamina b, whereas OFF-types arborize in sublamina a of the IPL (Famiglietti and Kolb, 1976; Nelson et al., 1978; Peichl and Wässle, 1981; Euler and Wässle, 1995; Hartveit, 1997). To date, three types of ON cone bipolar cells, calbindin-IR (Massey and Mills, 1996), CD15-IR (Brown and Masland, 1999), and NK1 receptor-IR (Casini et al., 2002) cone bipolar cells have been identified and well-characterized immunocytochemically. However, in the case of OFF-type cone bipolar cells only one variant, a recoverin-IR cone bipolar cell, has been reported (Massey and Mills, 1996). The HCN1-IR bipolar cells arborize in sublamina a of the IPL, and thus belong to OFF-type cone bipolar cells. We compared HCN1-IR bipolar cells with recoverin-IR OFF cone bipolar cells. Recoverin-IR OFF cone bipolar cells have axons branching and ramifying broadly through strata 1 and 2 of the IPL, whereas axons of the HCN1-IR bipolar cells ramified narrowly in the border of strata 1 and 2 of the IPL. In addition, HCN1-IR bipolar cells have lobular terminals, whereas axon terminals of the recoverin-IR OFF cone bipolar cells are not prominent. These different axonal morphologies suggest that HCN1-IR cone bipolar cells are OFF-type bipolar cells distinct from the recoverin-IR OFF-type bipolar cells.

Famiglietti (1981) classified rabbit bipolar cells using Golgi staining, and recently McGillem and Dacheux (2001) classified cone bipolar cells into 12 types by intracellular injection of the fluorescent dye Sulforhodamine B. Five different types of OFF cone bipolar cells were identified by Famiglietti (1981), and termed na1, na2, na3, ma, and wa. Three different types of OFF cone bipolar cells

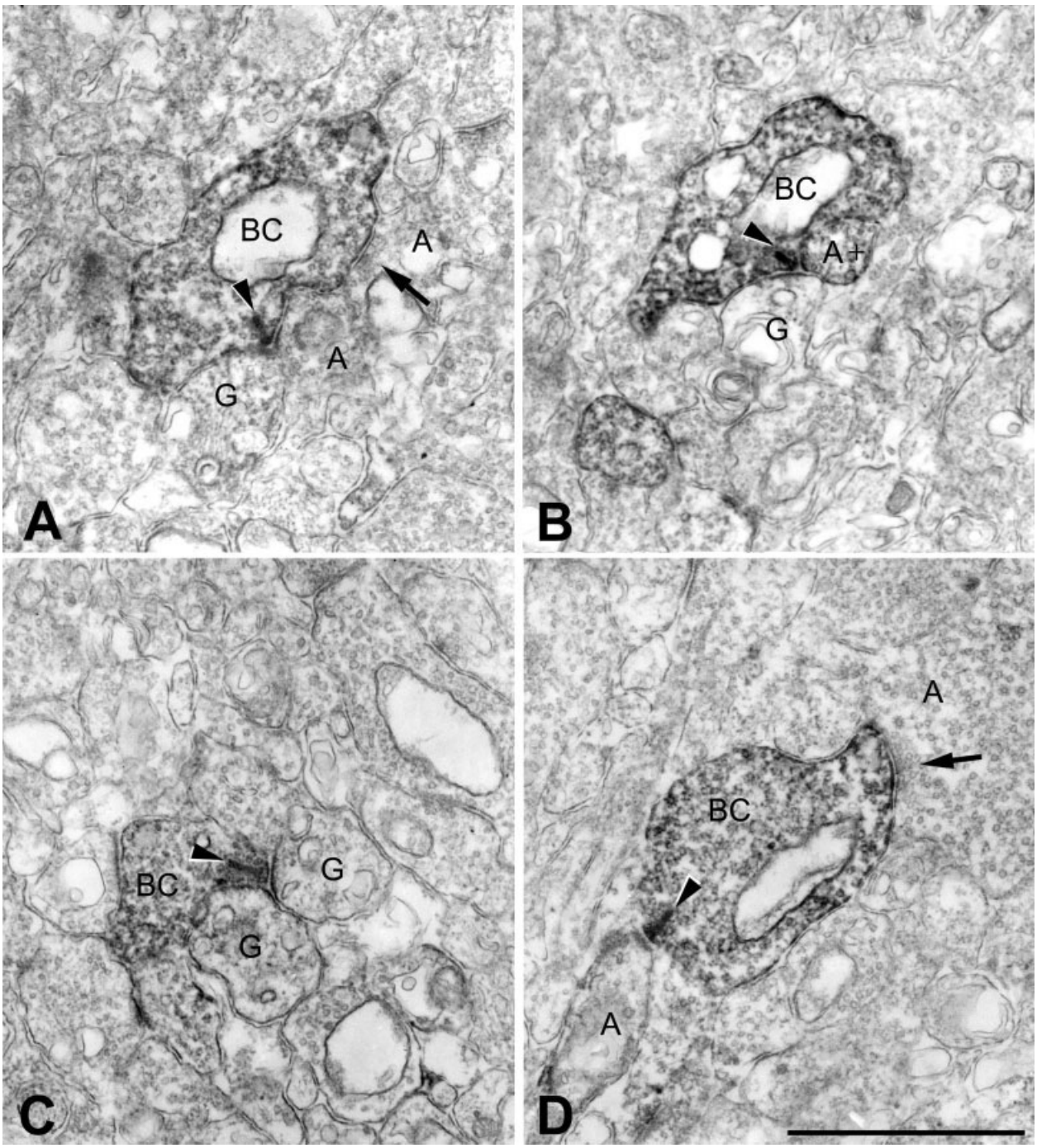

Fig. 6. Electron micrographs showing output synapses of HCN1-IR bipolar cells in sublamina a of the IPL. **A:** A labeled axon terminal makes a ribbon synapse (arrowhead). At the ribbon synapse, an amacrine process (A) and a ganglion cell dendrite (G) comprise a postsynaptic dyad. **B:** An axon terminal of an HCN1-labeled cone bipolar cell process (BC) makes a ribbon synapse (arrowhead) onto a postsynaptic dyad composed of a labeled amacrine cell process and a ganglion cell dendrite (G). **C:** An axon terminal of an HCN1-labeled cone bipolar cell process (BC) makes a ribbon synapse (arrowhead) onto a postsynaptic dyad composed of both ganglion cell dendrites (G). **D:** An amacrine cell process (A) forms a postsynaptic monad at the ribbon synapse (arrowhead) of an HCN1-labeled bipolar axon terminal (BC), which receives synaptic input (arrow) from another large amacrine cell process (A). Scale bar = 0.5 μm.

were identified and termed DAPI-Ba1, DAPI-Ba2, and DAPI-Ba3 (Mills and Massey, 1992). McGillem and Dacheux (2001) described six different types of OFF cone bipolar cells and termed them CBma1, CBwa1, CBna1-2, Cbma1-2, Cbna2, and Cbma2. In addition, they reported that CBma1, CBma2, and CBwa1 bipolar cells corre-

TABLE 1. Types and Frequencies of Synapses Made by HCN1-IR Bipolar Cells in the IPL of the Rabbit Retina[a]

		Number of synapses made by HCN1-IR bipolar cells
Presynaptic elements		
A− (rA−)[b]	59 (8)	98% (14%)
A+	1	2%
Subtotal	60	100%
Postsynaptic elements		
A−/A−	87	51%
A+/A−	1	<1%
A−/G	38	23%
A+/G	1	<1%
A−/U	25	15%
G/G	4	2%
G/U	10	6%
U/U	3	<2%
Total number of dyads	169	100%
A−/A−/G (triad)	1	
A−/U/U	1	
A− (monad)	5	
G	1	
Subtotal	177	
Total	237	

[a]Abbreviations: A+: HCN1-labeled amacrine cell; A−: unlabeled amacrine cell; G: ganglion cell; and U: unidentified cell.
[b]rA− represents unlabeled reciprocal amacrine cells and is included in A− category in this study.

sponded, respectively, to the DAPI-Ba1, DAPI-Ba2, and DAPI-Ba3 described by Mills and Massey (1992) or to types na2, na3, and ma of Famiglietti (1981). It is difficult to make an exact match with these classifications. However, it is possible that the HCN1-IR bipolar cell is equivalent to either the na2 or ma type of Famiglietti (1981), to the CBma1 or CBwa1 types of McGillem and Dacheux (2001) or to the DAPI-Ba1 or DAPI-Ba3 bipolar cells of Mills and Massey (1992)—equivalent to the DAPI-Ba1 type described by Mills and Massey (1992). This is based on the depth and morphology of the HCN1-IR bipolar cell axons, their cell density, and their synaptic circuitry. The aspects of cell density and synaptic circuitry of HCN1-IR bipolar cells are further discussed below.

Quantitative implication

The HCN1-IR bipolar cells formed a regular mosaic with a regularity ratio of 3.6 at a position 6 mm ventral to the optic disc. This ratio is similar to those for other bipolar populations in the rabbit retina, such as rod bipolar cells (5.1; Young and Vaney, 1991), DAPI-Ba1 cone bipolar cells (4.1; Mills and Massey, 1992), calbindin-IR cone bipolar cells (4.0–5.0; Massey and Mills, 1996), and NK1 receptor-IR cone bipolar cells (3.1–3.8; Casini et al., 2002). The peak density of HCN1-IR bipolar cells was 1,825 cells/mm^2 at a position 1 mm ventral to the visual streak and decreased with increasing eccentricity, reaching 650 cells/mm^2 at a position 13 mm ventral to the periphery. The peak density was estimated at 2,200 cells/mm^2 in the visual streak. These densities are similar to those of DAPI-Ba1 bipolar cells, which decreased in frequency from about 2,500 cells/mm^2 in the area of the visual streak to about 600 cells/mm^2 in the inferior periphery.

In the present study, the ratio of HCN1-IR bipolar cells to rod bipolar cells was 32–36% and was relatively constant across retinal regions. As the ratio of rod to cone bipolar cells is about 1:3 in the mid-inferior retina (Strettoi and Masland, 1995), the HCN1-IR bipolar cells thus constitute about 10% of the total cone bipolar cells in the mid-peripheral rabbit retina. This ratio is similar to or slightly higher than that of DAPI-Ba1 cone bipolar cells (7–8%; Mills and Massey, 1992), which are thought to be identical to the HCN1-IR bipolar cells. It is also similar to other cone bipolar populations in the rabbit retina, such as DAPI-Ba2 bipolar cells (6–10%; Mills and Massey, 1992), calbindin-IR cone bipolar cells (7–9%; Massey and Mills, 1996), CD15-IR cone bipolar cells (6–8%; Brown and Masland, 1999), and NK1 receptor-IR cone bipolar cells (10%; Casini et al., 2002).

In this study it was impossible to measure dendritic and axonal fields directly from individual HCN1-IR bipolar cells, and thus their dendritic and axonal fields were estimated on the assumption that the coverage of HCN1-IR bipolar cells is 1.0, based on previous reports (Young and Vaney, 1991; Mills and Massey, 1992; Brown and Masland, 1999). In this case, dendritic and axonal arbors are 25 μm in diameter near the visual streak and 40 μm at the periphery. In addition to the above assumption, a simple calculation from densities of about 10,000 cones/mm^2 at a position 6 mm ventral to the optic disc (Famiglietti and Sharpe, 1995) yields a potential convergence of 8.0 for cones to HCN1-IR bipolar cells. This number is between 7.4 for the visual streak and 10.3 for the inferior periphery for DAPI-Ba1 cone bipolar cell (Mills and Massey, 1992). Taken together, quantitative analysis suggests that the HCN1-IR bipolar cells are identical to the DAPI-Ba1 cone bipolar cells. However, more detailed studies combined with intracellular injection are needed to define the dendritic and axonal fields and coverage of the HCN1-IR bipolar cells.

Synaptic circuitry

In the present study, we confirmed the synaptic circuitry of the HCN1-IR bipolar cells. HCN1-IR bipolar cells belong to the flat variety, because all their dendrites examined with the electron microscope form basal junctions with cone pedicles. This is as expected from light microscopic observations that HCN1-IR bipolar cells terminate their axons on sublamina a of the IPL.

The cardinal feature of the synaptic circuitry of the HCN1-IR bipolar cell in the IPL is that the majority of both input and output synapses of their axons are with amacrine cells. There are two OFF-type cone bipolar cells in the rabbit retina, DAPI-Ba1 and DAPI-Ba2, for which synaptic circuits are known. In the IPL, the former type is pre- or postsynaptic to various types of amacrine cell processes of unknown origin, whereas the latter type is primarily presynaptic to ganglion cell dendrites and to reciprocal processes belonging to AII amacrine cells (Merighi et al., 1996). Thus, the synaptic circuitry of the HCN1-IR bipolar cell resembles that of the DAPI-Ba1-type bipolar cell in that the majority of pre- or postsynaptic elements are amacrine cell processes. However, in the present study 19% (57 cases) of identified postsynaptic elements (297 cases) were ganglion cell dendrites. These results are contrary to the report by Merighi et al. (1996), who have not been able to identify ganglion cell dendrites among the postsynaptic elements. This discrepancy might be due to the numbers of synapses examined.

Four kinds of amacrine cell processes have been described that might costratify with HCN1-IR bipolar axons: OFF-type starburst cholinergic amacrine cells (Famiglietti, 1983; Famiglietti and Tumosa, 1987; Vaney, 1990), distal processes of DAPI-3 amacrine cells (Vaney, 1990;

Wright et al., 1997), lobular appendages of AII amacrine cells (Famiglietti and Kolb, 1975; Strettoi et al., 1992), and the HCN1-IR amacrine cell processes introduced here. HCN1-IR amacrine cell processes that make pre- or postsynaptic contacts with HCN1-IR bipolar cell axons were observed only rarely. Pre- and postsynaptic amacrine cell processes showing the cytological characteristics of AII amacrine cells (Strettoi et al., 1992; Chun et al., 1993) were not frequently found, suggesting that the HCN1-IR cone bipolar cells are not a major population of cone bipolar cells as interneurons in the rod pathway in the rabbit retina. Thus, pre- or postsynaptic components of the HCN1-IR bipolar cells are presumably OFF-type starburst cholinergic amacrine cell processes and/or distal processes of DAPI-3 amacrine cells, which might be involved in a direction-selective (DS) mechanism. This argument is discussed in the following section.

Possible functions of the HCN1-IR cone bipolar cells

The DS mechanism is defined as the property of a cell that responds optimally to stimulus movement in a certain (preferred) direction, but is inhibited by movement in the opposite (null) direction. In the rabbit retina, there are two distinct types of DS ganglion cells that give either ON–OFF or ON–center responses to flashed illumination (Barlow et al., 1964). The more commonly encountered ON–OFF DS ganglion cells have a bistratified dendritic arbor, which is narrowly ramified within sublaminae a and b of the IPL, respectively (Amthor et al., 1984, 1989; Yang and Masland, 1994). The dendrites of ON–OFF DS ganglion cells costratify and cofasciculate with the processes of two types of amacrine cells termed ON- and OFF-type starburst amacrine cells (Famiglietti, 1981, 1983, 1992; Vaney et al., 1989; Vaney and Pow, 2000). Electron microscopy has shown that starburst amacrine cells synapse onto the ON–OFF DS ganglion cells (Famiglietti, 1991, 1992). In addition, certain types of cone bipolar cells give synaptic inputs onto both starburst amacrine and ON–OFF DS ganglion cells (Famiglietti, 1983, 1985b, 1991; Brandon 1987). Recently, one type of these cone bipolar cells, CD15-IR bipolar cell, has been characterized. These cells ramify their axons at the same level as the processes of ON-starburst amacrine cells and ON–OFF DS ganglion cells. Double-labeling confocal light microscopy has suggested that CD15-IR bipolar cells play a role in the ON–OFF DS neuronal circuitry (Brown and Masland, 1999). However, the OFF counterpart that might synapse onto both OFF-starburst amacrine and ON-OFF DS ganglion cells is still missing.

In this study, HCN1-IR bipolar cell axons were shown to ramify at the border of strata 1 and 2 of the IPL, where they formed a continuous beaded meshwork. This stratification level corresponds to that of processes of the OFF-type starburst cells (Famiglietti, 1983; Famiglietti and Tumosa, 1987; Vaney, 1990), to OFF-processes of the ON–OFF ganglion cells (Amthor et al., 1984, 1989; Yang and Masland, 1994), and to distal processes of the DAPI-3 amacrine cells (Vaney, 1990; Wright et al., 1997). These neurons might be involved in DS mechanisms in the rabbit retina. Double-labeling experiments showed that the HCN1-labeled bipolar cell axons stratified narrowly within and slightly proximal to the OFF-starburst amacrine cell processes and they followed OFF-type starburst amacrine cell processes, suggesting that both HCN1-IR bipolar cell axons and OFF-starburst amacrine cell processes are costratified and cofasciculated. In particular, their lobular axon terminals are exclusively located within the band of OFF-type starburst amacrine cell processes. In addition, both starburst amacrine and ON-OFF DS ganglion cells receive synaptic inputs from certain types of cone bipolar cells (Famiglietti, 1983, 1985b, 1991; Brandon 1987), and the present study showed that the majority of both input and output synapses of HCN1-IR bipolar axons are with amacrine cells. These results suggest that HCN1-IR bipolar cells might make contacts with OFF-type starburst amacrine cells. Taken together, HCN1-IR bipolar cells in this study may be involved in a DS mechanism, providing synaptic inputs onto the OFF circuit of DS in the same way as CD15-IR bipolar cells might be involved in the ON circuit.

LITERATURE CITED

Amthor FR, Oyster CW, Takahashi ES. 1984. Morphology of on-off direction-selective ganglion cells in the rabbit retina. Brain Res 298: 187–190.

Amthor FR, Takahashi ES, Oyster CW. 1989. Morphologies of rabbit retinal ganglion cells with complex receptive fields. J Comp Neurol 280:97–121.

Andressen C, Mai JK. 1997. Localization of the CD15 carbohydrate epitope in the vertebrate retina. Vis Neurosci 14:253–262.

Bader C, MacLeish P, Schwartz E. 1979. A voltage-clamp study of the light response in solitary rods of the tiger salamander. J Physiol 331:253–284.

Barlow HB, Hill RM, Levick WR. 1964. Retinal ganglion cells responding selectively to direction and speed of image motion in the rabbit. J Physiol 173:377–407.

Barnes S, Hille B. 1989. Ionic channels of the inner segment of tiger salamander cone photoreceptors. J Gen Physiol 94:719–743.

Boycott BB, Wässle H. 1991. Morphological classification of bipolar cells of the primate retina. Eur J Neurosci 3:1069–1088.

Brandon C. 1987. Cholinergic neurons in the rabbit retina: Dendritic branching and ultrastructural connectivity. Brain Res 426:119–130.

Brandstätter JH, Hack I. 2001. Localization of glutamate receptors at a complex synapse. The mammalian photoreceptor synapse. Cell Tiss Res 303:1–14.

Brown SP, Masland RH. 1999. Costratification of a population of bipolar cells with the direction-selective circuitry of the rabbit retina. J Comp Neurol 408:97–106.

Brown HF, DiFrancesco D, Noble SJ. 1979. How does adrenalin accelerate the heart? Nature 280:235–236.

Casini G, Sabatini A, Catalani E, Willems D, Bosco L, Brecha NC. 2002. Expression of the neurokinin 1 receptor in the rabbit retina. Neurosci 115:1309–1321.

Chun M-H, Han S-H, Chung J-W, Wässle H. 1993. Electron microscopic analysis of the rod pathway of the rat retina. J Comp Neurol 332:421–432.

Chun M-H, Kim I-B, Oh S-J, Chung J-W. 1999. Synaptic connectivity of two types of recoverin-labeled cone bipolar cells and glutamic acid decarboxylase immunoreactive amacrine cells in the inner plexiform layer of the rat retina. Vis Neurosci 16:791–800.

Cohen E, Sterling P. 1990. Demonstration of cell types among cone bipolar neurons of cat retina. Proc R Soc Lond B Biol Sci 330:305–321.

Demontis GC, Longoni B, Barcaro U, Cervetto L. 1999. Properties and functional roles of hyperpolarization-gated currents in guinea-pig retinal rods. J Physiol 515:813–828.

DiFrancesco D. 1981. A new interpretation of the pacemaker current in calf Purkinje fibres. J Physiol 314:359–376.

Dubin MW. 1970. The inner plexiform layer of the vertebrate retina: A quantitative and comparative electron microscopic analysis. J Comp Neurol 140:479–506.

Euler T, Wässle H. 1995. Immunocytochemical identification of cone bipolar cells in the rat retina. J Comp Neurol 361:461–478.

Fain G, Quandt F, Bastian B. 1978. Contribution of a caesium-sensitive conductance increase to the rod photoresponse. Nature 272:467–469.

Famiglietti EV. 1981. Functional architecture of cone bipolar cells in mammalian retina. Vision Res 21:1559–1563.

Famiglietti EV. 1983. ON and OFF pathways through amacrine cells in mammalian retina: the synaptic connection of "starburst" amacrine cells. Vision Res 23:1265–1279.

Famiglietti EV. 1985a. Starburst amacrine cells: morphological constancy and systematic variation in the anisotropic field of rabbit retinal neurons. J Neurosci 5:562–577.

Famiglietti EV. 1985b. Synaptic organization of ON-OFF directionally selective ganglion cells in rabbit retina. Soc Neurosci Abst 11:337.

Famiglietti EV. 1991. Synaptic organization of starburst amacrine cells in rabbit retina: analysis of serial thin sections by electron microscopy and graphic reconstruction. J Comp Neurol 309:40–70.

Famiglietti EV. 1992. Dendritic co-stratification of ON and ON-OFF directionally selective ganglion cells with starburst amacrine cells in rabbit retina. J Comp Neurol 324:322–335.

Famiglietti EV, Kolb H. 1975. A bistratified amacrine cell and synaptic circuitry in the inner plexiform layer of the retina. Brain Res 84:293–300.

Famiglietti EV, Kolb H. 1976. Structural basis for ON- and OFF-center responses in retinal ganglion cells. Science 194:193–195.

Famiglietti EV, Sharpe SJ. 1995. Regional topography of rod and immunocytochemically characterized 'blue' and 'green' cone photoreceptors in rabbit retina. Vis Neurosci 12:1151–1175.

Famiglietti EV, Tumosa N. 1987. Immunocytochemical staining of cholinergic amacrine cells in rabbit retina. Brain Res 413:398–403.

Gargini C, Demontis GC, Bisti S, Cervetto L. 1999. Effects of blocking the hyperpolarization-activated current (I_h) on the cat electroretinogram. Vision Res 39:1767–1774.

Gauss R, Seifert R, Kaupp UB. 1998. Molecular identification of a hyperpolarization-activated channel in sea urchin sperm. Nature 393: 583–587.

Greferath U, Grünert U, Wässle H. 1990. Rod bipolar cells in the mammalian retina show protein kinase C-like immunoreactivity. J Comp Neurol 301:433–442.

Grünert U, Martin P. 1991. Rod bipolar cells in the macaque monkey retina: Immunoreactivity and connectivity. J Neurosci 11:2742–2758.

Grünert U, Martin P, Wässle H. 1994. Immunocytochemical analysis of bipolar cells in the macaque monkey retina. J Comp Neurol 348:607–627.

Hartveit E. 1997. Functional organization of cone bipolar cells in the rat retina. J Neurophysiol 4:1716–1730.

Hestrin S. 1987. The properties and function of inward rectification in rod photoreceptors of the tiger salamander. J Physiol 390:319–333.

Kim I-B, Lee E-J, Kim M-K, Park D-K, Chun M-H. 2000. Choline acetyltransferase-immunoreactive neurons in the developing rat retina. J Comp Neurol 427:604–616.

Kim I-B, Lee E-J, Oh S-J, Park C-B, Pow DV, Chun M-H. 2002. Light and electron microscopic analysis of aquaporin 1-like-immunoreactive amacrine cells in the rat retina. J Comp Neurol 452:178–191.

Kolb H. 1979. The inner plexiform layer in the retina of the cat: electron microscopic observations. J Neurocytol 8:295–329.

Kolb H, Nelson R, Mariani A. 1981. Amacrine cells, bipolar cells and ganglion cells of the cat retina: a Golgi study. Vision Res 21:1081–1114.

Kolb H, Linberg KA, Fisher SK. 1992. Neurons of the human retina: a Golgi study. J Comp Neurol 318:147–187.

Lambrecht H-G, Koch K-W. 1992. Recoverin, a novel calcium binding protein from vertebrate photoreceptors. Biochim Biophys Acta 1160: 63–66.

Ludwig A, Zong X, Jeglitsch M, Hofmann F, Biel M. 1998. A family of hyperpolarization-activated mammalian cation channels. Nature 393: 587–591.

Ludwig A, Zong X, Stieber J, Hullin R, Hofmann F, Biel M. 1999. Two pacemaker channels from human heart with profoundly different activation kinetics. EMBO J 18:2323–2329.

Massey SC, Mills SL. 1996. A calbindin-immunoreactive cone bipolar cell type in the rabbit retina. J Comp Neurol 355:15–33.

McGillem GS, Dacheux RF. 2001. Rabbit cone bipolar cells: correlation of their morphologies with whole-cell recordings. Vis Neurosci 18:675–685.

McGuire BA, Stevens JK, Sterling P. 1984. Microcircuitry of bipolar cells in cat retina. J Neurosci 4:2920–2938.

McGuire BA, Stevens JK, Sterling P. 1986. Microcircuitry of beta ganglion cells in cat retina. J Neurosci 6:907–918.

Merighi A, Raviola E, Dacheux RF. 1996. Connections of two types of flat cone bipolars in the rabbit retina. J Comp Neurol 371:164–178.

Milam AH, Dacey DM, Dizhoor AM. 1993. Recoverin immunoreactivity in mammalian cone bipolar cells. Vis Neurosci 10:1–13.

Mills SL, Massey SC. 1992. Morphology of bipolar cells labeled by DAPI in the rabbit retina. J Comp Neurol 321:133–149.

Moosmang S, Stieber J, Zong X, Biel M, Hofmann F, Ludwig A. 2001. Cellular expression and functional characterization of four hyperpolarization-activated pacemaker channels in cardiac and neuronal tissues. Eur J Biochem 268:1646–1652.

Müller F, Scholten A, Ivanova E, Haverkamp S, Kremmer E, Grünert U, Kaupp B. 2001. HCN channels in the mammalian retina. Soc Neurosci Abst 27:284.6.

Müller F, Scholten A, Ivanova E, Haverkamp S, Kremmer E, Kaupp UB. 2003. HCN channels are expressed differentially in retinal bipolar cells and concentrated at synaptic terminals. Eur J Neurosci 17:2084–2096.

Negishi K, Kato S, Teranishi T. 1988. Dopamine cells and rod bipolar cells contain protein kinase C-like immunoreactivity in some vertebrate retinas. Neurosci Lett 94:247–252.

Nelson R, Kolb H. 1983. Synaptic patterns and response properties of bipolar and ganglion cells in the cat retina. Vision Res 23:1183–1195.

Nelson R, Famiglietti EV, Kolb H. 1978. Intracellular staining reveals different levels of stratification for on-center and off-center ganglion cells in the cat retina. J Neurophysiol 4:427–483

Pape HC. 1996. Queer current and pacemaker: the hyperpolarization-activated cation current in neurons. Annu Rev Physiol 58:299–327.

Ribak CE, Tong WMY, Brecha NC. 1996. GABA plasma membrane transporters, GAT-1 and GAT-3, display different distributions in the rat hippocampus. J Comp Neurol 367:595–606.

Röhrenbeck J, Wässle H, Boycott BB. 1989. Horizontal cells in the monkey retina: immunocytochemical staining with antibodies against calcium binding proteins. Eur J Neurosci 1:407–420.

Santoro B, Liu DT, Yao H, Bartsch D, Kandel ER, Siegelbaum SA, Tibbs GR. 1998. Identification of a gene encoding a hyperpolarization-activated pacemaker channel of brain. Cell 93:717–729.

Seifert R, Scholten A, Gauss R, Mincheva A, Lichter P, Kaupp UB. 1999. Molecular characterization of a slowly gating human hyperpolarization-activated channel predominantly expressed in thalamus, heart, and testis. Proc Natl Acad Sci U S A 96:9391–9396.

Strettoi E, Masland RH. 1995. The organization of the inner nuclear layer of the rabbit retina. J Neurosci 15:875–888.

Strettoi E, Raviola E, Dacheux RF. 1992. Synaptic connections of the narrow-field bistratified rod amacrine cell (AII) in the rabbit retina. J Comp Neurol 325:152–168.

Vaney DI. 1990. The mosaic of amacrine cells in the mammalian retina. Prog Ret Res 9:49–100.

Vaney DI, Pow DV. 2000. The dendritic architecture of the cholinergic plexus in the rabbit retina: selective labeling by glycine accumulation in the presence of sarcosine. J Comp Neurol 421:1–13.

Vaney DI, Collin SP, Young HM. 1989. Dendritic relationships between cholinergic amacrine cells and direction-selective ganglion cells. In: Weiler R, Osborne NN, editors. Neurobiology of the inner retina. Berlin: Springer. p 157–168.

Wässle H, Riemann HJ. 1978. The mosaic of nerve cells in the mammalian retina. Proc R Soc Lond B Biol Sci 200:441–461.

Wright LL, Macqueen CL, Elston GN, Young HM, Pow DV, Vaney DI. 1997. The DAPI-3 amacrine cells of the rabbit retina. Vis Neurosci 14:473–492.

Yanagihara K, Irisawa H. 1980. Inward current activated during hyperpolarization in the rabbit sinoatrial node cell. Pfluegers Arch 388:11–19.

Yang G, Masland RH. 1994. Receptive fields and dendritic structure of directionally selective retinal ganglion cells. J Neurosci 14:5267–5280.

Young HM, Vaney DI. 1991. Rod-signal interneurons in the rabbit retina. 1. Rod bipolar cells. J Comp Neurol 310:139–153.